mathematics

Article

On the Dynamic Geometry of Kasner Quadrilaterals with Complex Parameter

Dorin Andrica [1] and Ovidiu Bagdasar [2,3,*]

[1] Faculty of Mathematics and Computer Science, Babeş-Bolyai University, 400084 Cluj-Napoca, Romania
[2] School of Computing and Engineering, University of Derby, Derby DE22 1GB, UK
[3] Department of Mathematics, Faculty of Exact Sciences, "1 Decembrie 1918" University of Alba Iulia, 510009 Alba Iulia, Romania
* Correspondence: o.bagdasar@derby.ac.uk

Abstract: We explore the dynamics of the sequence of Kasner quadrilaterals $(A_nB_nC_nD_n)_{n\geq 0}$ defined via a complex parameter α. We extend the results concerning Kasner triangles with a fixed complex parameter obtained in earlier works and determine the values of α for which the generated dynamics are convergent, divergent, periodic, or dense.

Keywords: dynamical systems; Kasner quadrilaterals; convergence; orbits; nested quadrilaterals

MSC: 51P99; 60A99

check for updates

Citation: Andrica, D.; Bagdasar, O. Dynamic Geometry of Kasner Quadrilaterals with Complex Parameter. *Mathematics* **2022**, *10*, 3334. https://doi.org/10.3390/math10183334

Academic Editors: Valer-Daniel Breaz and Ioan-Lucian Popa

Received: 10 August 2022
Accepted: 10 September 2022
Published: 14 September 2022

1. Introduction

For a real number α and an initial quadrilateral $A_0B_0C_0D_0$, one can construct the quadrilateral $A_1B_1C_1D_1$ such that A_1, B_1, C_1, and D_1 divide the segments $[A_0B_0]$, $[B_0C_0]$, $[C_0D_0]$, and $[D_0A_0]$, respectively, in the ratio $1-\alpha : \alpha$. Continuing this process, one obtains the terms $A_nB_nC_nD_n$, $n \geq 0$ whose terms are referred to as Kasner (or nested) quadrilaterals (after E. Kasner (1878–1955) who initiated these studies). A natural problem is to find the numbers α for which the sequence $(A_nB_nC_nD_n)_{n\geq 0}$ is convergent.

The related dynamic geometries inspired by simple iterations (especially for triangles) are reviewed in the article [1]:

generated by the incircle and the circumcircle of a triangle, the pedal triangle [2], the orthic triangle, and the incentral triangle. Similar recursive systems describing dynamic geometries are considered by S. Abbot [3], G. Z. Chang and P. J. Davis [4], R. J. Clarke [5], J. Ding, L. R. Hitt, and X-M. Zhang [6], L. R. Hitt and X-M. Zhang [7], and D. Ismailescu and J. Jacobs [8], or in the works by Dionisi et al. [9] and Roeschel [10]. In the paper [1], we proved that the sequence of Kasner triangles is convergent if and only if $\alpha \in (0,1)$, also providing the order of convergence.

Here, we prove similar results for the Kasner quadrilaterals, given by the complex coordinates of their vertices $A_n(a_n)$, $B_n(b_n)$, $C_n(c_n)$, $D_n(c_n)$, $n \geq 0$ (see the notation in [11]). The iterations are defined recursively for $n \geq 0$ as:

$$\begin{cases} a_{n+1} = \alpha a_n + (1-\alpha)b_n \\ b_{n+1} = \alpha b_n + (1-\alpha)c_n \\ c_{n+1} = \alpha c_n + (1-\alpha)d_n \\ d_{n+1} = \alpha d_n + (1-\alpha)a_n. \end{cases} \tag{1}$$

In this paper, we investigate the dynamic geometry generated by the sequence $(A_nB_nC_nD_n)_{n\geq 0}$, when α is a complex number. Notice that when α is complex, the quadrilaterals $A_nB_nC_nD_n$ are not always nested. The work extends results for triangles in [12], preparing the ground for the study of the general case of Kasner polygons.

2. Preliminaries

The system (1) can be written in matrix form as

$$X_{n+1} = \begin{pmatrix} a_{n+1} \\ b_{n+1} \\ c_{n+1} \\ d_{n+1} \end{pmatrix} = \begin{pmatrix} \alpha & 1-\alpha & 0 & 0 \\ 0 & \alpha & 1-\alpha & 0 \\ 0 & 0 & \alpha & 1-\alpha \\ 1-\alpha & 0 & 0 & \alpha \end{pmatrix} \begin{pmatrix} a_n \\ b_n \\ c_n \\ d_n \end{pmatrix} = TX_n, \tag{2}$$

where $X_n = (a_n, b_n, c_n, d_n)^T$, $n \geq 0$. In this notation, one can write

$$X_n = T^n X_0. \tag{3}$$

The matrix T has the characteristic polynomial

$$\begin{aligned} p_T(u) &= (u-\alpha)^4 - (1-\alpha)^4 \\ &= u^4 - 4u^3\alpha + 6u^2\alpha^2 - 6u\alpha^3 + \alpha^4 - (1-\alpha)^4 \\ &= (u-1)(u-2\alpha+1)\Big(u^2 - 2\alpha u + 2\alpha^2 - 2\alpha + 1\Big), \end{aligned}$$

whose roots can be written as $u_0 = 1$ and

$$u_1 = \alpha + (1-\alpha)\,i = (1-i)\left(\alpha - \frac{1-i}{2}\right) \tag{4}$$

$$u_2 = \alpha - (1-\alpha) = 2\left(\alpha - \frac{1}{2}\right) \tag{5}$$

$$u_3 = \alpha - (1-\alpha)\,i = (1+i)\left(\alpha - \frac{1+i}{2}\right). \tag{6}$$

A direct computation shows that

$$T = F^{-1} \begin{pmatrix} 1 & 0 & 0 & 0 \\ 0 & u_1 & 0 & 0 \\ 0 & 0 & u_2 & 0 \\ 0 & 0 & 0 & u_3 \end{pmatrix} F, \tag{7}$$

where the matrices F and F^{-1} are given by

$$F = \begin{pmatrix} 1 & 1 & 1 & 1 \\ 1 & -i & -1 & i \\ 1 & -1 & 1 & -1 \\ 1 & i & -1 & -i \end{pmatrix}, \quad F^{-1} = \frac{1}{4} \begin{pmatrix} 1 & 1 & 1 & 1 \\ 1 & i & -1 & -i \\ 1 & -1 & 1 & -1 \\ 1 & -i & -1 & i \end{pmatrix}. \tag{8}$$

By using (7), for every positive integer n, we have the following relations

$$\begin{aligned} T^n &= F^{-1} \begin{pmatrix} 1 & 0 & 0 & 0 \\ 0 & u_1^n & 0 & 0 \\ 0 & 0 & u_2^n & 0 \\ 0 & 0 & 0 & u_3^n \end{pmatrix} F \\ &= \frac{1}{4} \begin{pmatrix} 1 & 1 & 1 & 1 \\ 1 & i & -1 & -i \\ 1 & -1 & 1 & -1 \\ 1 & -i & -1 & i \end{pmatrix} \begin{pmatrix} 1 & 0 & 0 & 0 \\ 0 & u_1^n & 0 & 0 \\ 0 & 0 & u_2^n & 0 \\ 0 & 0 & 0 & u_3^n \end{pmatrix} \begin{pmatrix} 1 & 1 & 1 & 1 \\ 1 & -i & -1 & i \\ 1 & -1 & 1 & -1 \\ 1 & i & -1 & -i \end{pmatrix}. \end{aligned} \tag{9}$$

By Formula (3), one obtains

$$\begin{aligned} a_n &= g_0 + Mu_1^n + Nu_2^n + Pu_3^n \\ b_n &= g_0 + (Mi)u_1^n + (-N)u_2^n + (-Pi)u_3^n \\ c_n &= g_0 + (-M)u_1^n + Nu_2^n + (-P)u_3^n \\ d_n &= g_0 + (-Mi)u_1^n + (-N)u_2^n + (Pi)u_3^n, \end{aligned} \tag{10}$$

where $g_0 = \frac{a_0+b_0+c_0+d_0}{4}$, where multiplying (9) by $(a_0, b_0, c_0, d_0)^T$ we obtain

$$M = \frac{a_0 - b_0 i - c_0 + d_0 i}{4}, \quad N = \frac{a_0 - b_0 + c_0 - d_0}{4}, \quad P = \frac{a_0 + b_0 i - c_0 - d_0 i}{4}. \tag{11}$$

From these formulae (but also from (1)), notice that $a_n + b_n + c_n + d_n = 4g_0$, $n \geq 0$; hence, all polygons $A_nB_nC_nD_n$ have the same centroid G_0. Clearly, when $M, N, P \neq 0$, the terms u_1^n, u_2^n, and u_3^n appear explicitly in (10).

3. Dynamical Properties in the Case of Real Parameter

In this section, we study the convergence of the sequence of the Kasner quadrilaterals when α is a real number. By Formula (10), the sequences $(a_n)_{n\geq 0}$, $(b_n)_{n\geq 0}$, $(c_n)_{n\geq 0}$, and $(d_n)_{n\geq 0}$ are convergent if and only if $|u_1| < 1$, $|u_2| < 1$, and $|u_3| < 1$, that is,

$$\begin{aligned} |u_1| &= \left|(1-i)\left(\alpha - \frac{1-i}{2}\right)\right| = \sqrt{2}\left|\alpha - \frac{1-i}{2}\right| < 1, \\ |u_2| &= 2\left|\alpha - \frac{1}{2}\right| < 1, \\ |u_3| &= \left|(1+i)\left(\alpha - \frac{1+i}{2}\right)\right| = \sqrt{2}\left|\alpha - \frac{1+i}{2}\right| < 1. \end{aligned} \tag{12}$$

First, one can easily check that the condition $|u_2| < 1$ is equivalent to $\alpha \in (0,1)$.

Then, because α is real, we clearly have $|u_1| = |u_3|$; hence, the conditions $|u_1| < 1$ and $|u_3| < 1$ become equivalent to $|u_1u_3| < 1$, that is,

$$|u_1u_3| = 2\left|\alpha - \frac{1-i}{2}\right|\left|\alpha - \frac{1+i}{2}\right| = 2\left(\alpha^2 - \alpha + \frac{1}{2}\right) < 1,$$

which is equivalent to $\alpha(1-\alpha) < 0$, that is, $\alpha \in (0,1)$.

4. Dynamical Properties in the Case of Complex Parameter

We now discuss the dynamics obtained when α is a complex number.

It is convenient to define the following points

$$z_1 = \frac{1}{2} - \frac{1}{2}i, \quad z_2 = \frac{1}{2}, \quad z_3 = \frac{1}{2} + \frac{1}{2}i, \tag{13}$$

representing the centres of the open disks

$$D_1\left(z_1, \frac{\sqrt{2}}{2}\right), \quad D_2\left(z_2, \frac{1}{2}\right), \quad D_3\left(z_3, \frac{\sqrt{2}}{2}\right), \tag{14}$$

and of the circles depicted in Figure 1

$$C_1\left(z_1, \frac{\sqrt{2}}{2}\right), \quad C_2\left(z_2, \frac{1}{2}\right), \quad C_3\left(z_3, \frac{\sqrt{2}}{2}\right). \tag{15}$$

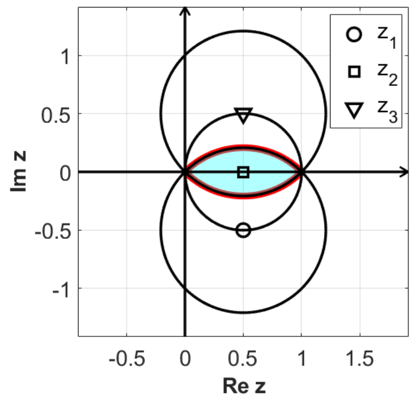

Figure 1. Plots of the circles C_1, C_2, and C_3 defined in Formula (15).

Considering the real numbers $r_1, r_2, r_3, \theta_1, \theta_2, \theta_3$, by (4), (5), and (6), we obtain

$$\begin{aligned} u_1 &= r_1 e^{2\pi i \theta_1} = \sqrt{2}(\alpha - z_1) e^{-\frac{\pi i}{4}}, \\ u_2 &= r_2 e^{2\pi i \theta_2} = 2(\alpha - z_2), \\ u_3 &= r_3 e^{2\pi i \theta_3} = \sqrt{2}(\alpha - z_3) e^{\frac{\pi i}{4}}. \end{aligned} \tag{16}$$

By (16), we deduce that for a given $j = 1, 2, 3$, if $\alpha \in D_j$, then we have $r_j < 1$. Moreover, if $\alpha \in C_j$, then it follows that $r_j = 1$. The distinct behaviours below emerge:

1. If $\alpha \in D_1 \cap D_2 \cap D_3$, then $0 < r_1, r_2, r_3 < 1$.
   One can easily check the set inclusion $D_1 \cap D_3 \subseteq D_2$.
2. If α is in the interior of the complement of $D_1 \cap D_3$, then $\max\{r_1, r_3\} > 1$.
3. If $\alpha \in C_1 \cap C_2 \cap C_3$, then $\alpha \in \{0, 1\}$.

The boundary of the shaded region in Figure 1 consists of two arcs

$$U_1 = C_1 \cap D_3, \quad U_3 = C_3 \cap D_1,$$

which can be parametrised as

$$\alpha(t) = \begin{cases} z_1 + \frac{\sqrt{2}}{2}(\cos t + i \sin t), & t \in \left[\frac{\pi}{4}, \frac{3\pi}{4}\right] \\ z_3 + \frac{\sqrt{2}}{2}(\cos t + i \sin t), & t \in \left[\frac{5\pi}{4}, \frac{7\pi}{4}\right]. \end{cases} \tag{17}$$

To describe the orbits of the sequences $(a_n)_{n \geq 0}$, $(b_n)_{n \geq 0}$, $(c_n)_{n \geq 0}$, and $(d_n)_{n \geq 0}$, one first needs to understand the behaviour of the sequence $(z^n)_{n \geq 0}$, where $z \in \mathbb{C}$ (see, for example, Lemma 2.1 in [13], or Lemma 5.2 in [14]), which is shown in Figure 2.

Lemma 1. *Let $z = re^{2\pi i \theta}$, where $r \geq 0$, $\theta \in \mathbb{R}$. The orbit of $(z^n)_{n \geq 0}$ is:*
(a) A spiral convergent to 0 for $r < 1$;
(b) A divergent spiral for $r > 1$;
(c) A regular $k-$gon if z is a primitive $k-$th root of unity, $k \geq 3$;
(d) A dense subset of the unit circle if $r = 1$ and $\theta \in \mathbb{R} \setminus \mathbb{Q}$.
When $\theta = j/k \in \mathbb{Q}$ is irreducible, then the terms of the spirals obtained in (a) and (b) align along k rays.

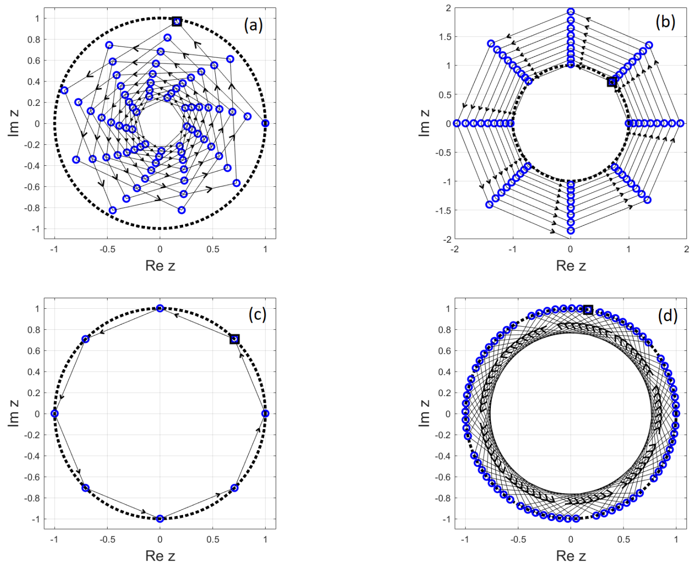

Figure 2. The terms z^n, $n = 0, \ldots, 70$ obtained for (**a**) $r = 0.98$ and $x = \sqrt{5}/10$; (**b**) $r = 1.01$ and $x = 1/8$; (**c**) $r = 1$ and $x = 1/8$; (**d**) $r = 1$ and $x = \sqrt{5}/10$. Arrows indicate the orbit's direction, and the dotted line represents the unit circle. The point $z = r\exp(2\pi i x)$ is shown as a square.

To prove part (d), we use that $z^n = e^{2\pi i\, n\theta} = e^{2\pi i\,(n\theta+m)}$ for $n \geq 0$ and m integers. By Kronecker's Lemma ([15], Theorem 442), the set $\{n\theta + m : m, n \in \mathbb{Z}, n \geq 0\}$ is dense in the set of real numbers $\mathbb{R}$; hence, the set $\{z^n : n \geq 0\}$ is dense within the unit circle.

As linear combinations of $(u_1^n)_{n\geq 0}$, $(u_2^n)_{n\geq 0}$, and $(u_3^n)_{n\geq 0}$, the sequences $(a_n)_{n\geq 0}$, $(b_n)_{n\geq 0}$, $(c_n)_{n\geq 0}$, and $(d_n)_{n\geq 0}$, given by the explicit Formula (10) in the complex plane, exhibit the following behaviour.

Lemma 2. *The patterns produced by Formula (10) are summarized below:*

1. *Convergent if* $0 < r_1, r_2, r_3 < 1$*;*
2. *Divergent if* $\max\{r_1, r_3\} > 1$*;*
3. *Periodic if* $r_1 = r_3 = 1$ *(that is, when* $\alpha = 0$ *or* $\alpha = 1$*);*
4. *There are two distinct patterns when* $0 < \min\{r_1, r_3\} < \max\{r_1, r_3\} = 1$*.*
   Denoting $\theta = \theta_1$ *if* $r_1 = 1$ *or* $\theta = \theta_3$ *if* $r_3 = 1$*, then the orbit:*
   (a) *Has k convergent subsequences if* $\theta = \frac{j}{k}$ *is an irreducible fraction;*
   (b) *Is dense within a circle when* θ *is irrational.*

The details of the geometric patterns obtained in each case are presented below. In all figures, we consider the initial polygon of complex coordinates

$$A_0(-4 + 12i), \quad B_0(0), \quad C_0(8), \quad D_0(12 + 1i), \tag{18}$$

for which Formula (11) gives the values

$$G = 4 + 5i, \quad M = -5 + 6i, \quad N = -2 + i, \quad P = -1. \tag{19}$$

The position of α relative to relevant boundaries is indicated in the left diagram with a star, while the iterations of the polygon are displayed on the right, where the star indicates the position of the centroid. All the simulations have been implemented in Matlab® 2021b.

4.1. Convergent Orbits

If $0 < r_1, r_2, r_3 < 1$, then by (16), the sequences u_1^n, u_2^n, and u_3^n are convergent if and only if $\alpha \in D_1 \cap D_3$. Hence, by (10), we obtain that $(a_n)_{n\geq 0}$, $(b_n)_{n\geq 0}$, $(c_n)_{n\geq 0}$, and $(d_n)_{n\geq 0}$ converge to g_0. We can formulate the following result.

Theorem 1. *The following assertions hold:*

(1) *The sequence $(A_nB_nC_nD_n)_{n\geq 0}$ is convergent if and only if $\alpha \in D_1 \cap D_2$.*
(2) *When the sequence $(A_nB_nC_nD_n)_{n\geq 0}$ is convergent, its limit is the degenerated quadrilateral at G_0, the centroid of the initial quadrilateral $A_0B_0C_0D_0$.*

Proof. The intersection $D_1 \cap D_3$ is shaded in Figure 1.

(1) Clearly, $\alpha \in D_1 \cap D_3$ is equivalent to $r_1 < 1$ and $r_3 < 1$ (in this case, one also has $\alpha \in D_2$). The relation (10) shows that the sequences $(a_n)_{n\geq 0}$, $(b_n)_{n\geq 0}$, $(c_n)_{n\geq 0}$, and $(d_n)_{n\geq 0}$ are convergent if and only if $(u_1^n)_{n\geq 0}$, $(u_2^n)_{n\geq 0}$, and $(u_3^n)_{n\geq 0}$ are convergent, which happens when $u_1^n \to 0$, $u_2^n \to 0$, and $u_3^n \to 0$.

(2) Adding the equation in the system (1), one obtains that for every integer $n \geq 0$, we have $a_n + b_n + c_n + d_n = a_0 + b_0 + c_0 + d_0 = 4g_0$, where g_0 is the complex coordinates of the centroid G_0 of the initial quadrilateral $A_0B_0C_0D_0$. Assume that $a_n \to a^*$, $b_n \to b^*$, $c_n \to c^*$, and $d_n \to d^*$. From system (1), we obtain

$$\begin{cases} a^* = \alpha a^* + (1-\alpha)b^* \\ b^* = \alpha b^* + (1-\alpha)c^* \\ c^* = \alpha c^* + (1-\alpha)d^* \\ d^* = \alpha d^* + (1-\alpha)a^*. \end{cases} \tag{20}$$

Because $\alpha \neq 1$, the only solution of this system is $a^* = b^* = c^* = d^* = g_0$. $\square$

For $0 < \alpha < 1$, one has $\alpha \in D_1 \cap D_3$, and moreover, in this case, the vertices A_{n+1}, B_{n+1}, C_{n+1}, D_{n+1} are interior points of the segments $[A_n, B_n]$, $[B_n, C_n]$, $[C_n, D_n]$, and $[D_n, A_n]$, respectively. Such an example is depicted in Figure 3.

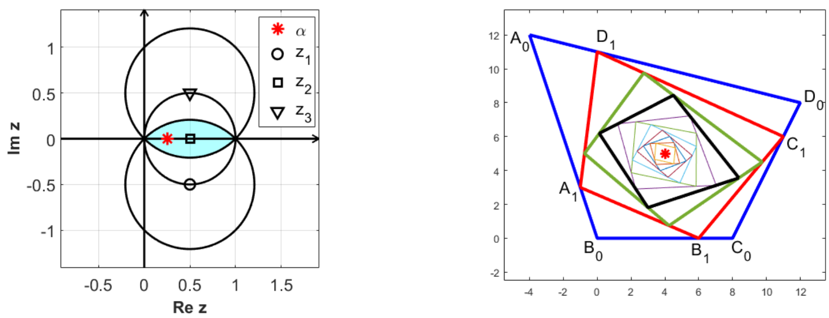

Figure 3. Convergent orbits (**right**) obtained for $\alpha = 0.25$ (**left**).

On the other hand, when the parameter $\alpha \in D_1 \cap D_3$ is not real, the orbit is convergent, but the points are not aligned any more, as illustrated in Figure 4.

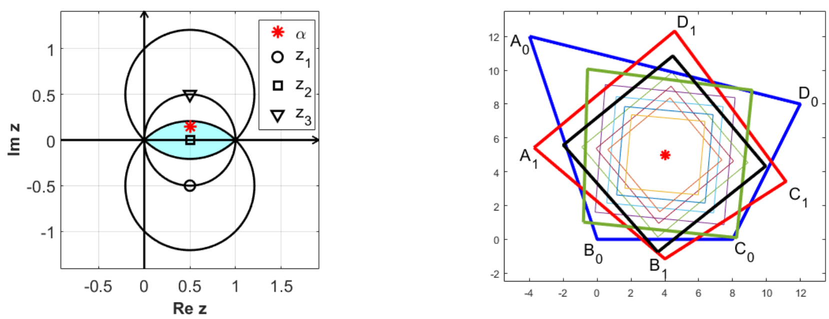

Figure 4. Convergent orbits (**right**) obtained for $\alpha = \frac{1}{2} + \frac{\sqrt{3}}{12}i$ (**left**).

4.2. Periodic Orbits

If $r_1 = r_2 = r_3 = 1$, then $|\alpha - z_1| = |\alpha - z_3| = \frac{\sqrt{2}}{2}$ and $|\alpha - z_2| = \frac{1}{2}$, which can only happen for $\alpha \in C_1 \cap C_2 \cap C_3 = \{0, 1\}$.

Case 1. $\alpha = 0$. From the system (1), for all $n \geq 0$, one obtains

$$a_{n+4} = b_{n+3} = c_{n+2} = d_{n+1} = a_n.$$

Similarly, $b_{n+4} = b_n$, $c_{n+4} = c_n$, and $d_{n+4} = d_n$, so the sequence terms satisfy

$$\begin{cases} a_n : & a_0, b_0, c_0, d_0, a_0, b_0, c_0, \ldots \\ b_n : & b_0, c_0, d_0, a_0, b_0, c_0, d_0, \ldots \\ c_n : & c_0, d_0, a_0, b_0, c_0, d_0, a_0, \ldots \\ d_n : & d_0, a_0, b_0, c_0, d_0, a_0, b_0, \ldots . \end{cases} \tag{21}$$

Case 2. $\alpha = 1$. From the system (1), for all $n \geq 0$, one obtains

$$a_{n+1} = a_n, \quad b_{n+1} = b_n, \quad c_{n+1} = c_n, \quad d_{n+1} = d_n,$$

so, in this case, the sequences are actually constant.

4.3. Divergent Orbits

If $\max\{r_1, r_3\} > 1$, then $\alpha \in \operatorname{int}\left[(D_1 \cap D_3)^c\right]$; hence, by (16), either u_1^n or u_3^n are divergent. By Formula (10), the sequences $(a_n)_{n\geq 0}$, $(b_n)_{n\geq 0}$, $(c_n)_{n\geq 0}$, and $(d_n)_{n\geq 0}$ are divergent (as long as the corresponding coefficients M, N, P in (10) are not all vanishing).

Figure 5 shows a divergent iteration. The diagram on the left we plot the position of α, while on the right side we illustrate the polygons $A_nB_nC_nD_n$, $n = 0, \ldots, 10$.

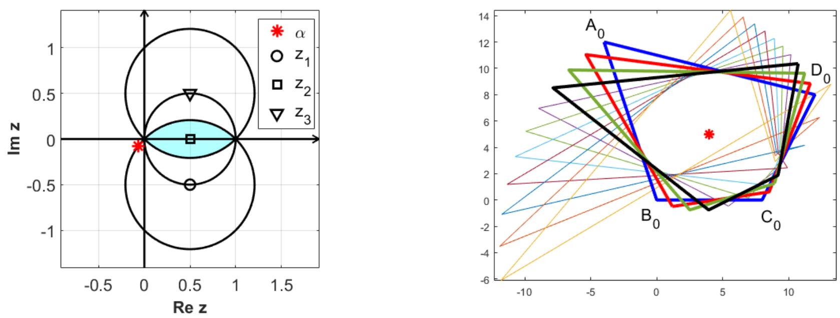

Figure 5. Divergent orbits (**right**) obtained for $\alpha = z_1 + \frac{\sqrt{2}}{2}(\cos 2.5 + i \sin 2.5)$ (**left**).

4.4. Orbits with a Finite Number of Convergent Subsequences

If $0 < \min\{r_1, r_3\} < \max\{r_1, r_3\} = 1$, then one either has $\alpha \in C_1 \cap D_3$ for $r_1 = 1$, or $\alpha \in C_3 \cap D_1$ for $r_3 = 1$. The orbit has a finite number of limit points if the complex argument θ of u_1 if $r_1 = 1$ or of u_3 if $r_3 = 1$ is rational.

4.4.1. Upper Arc of C_1

First, assume that $r_1 = \max\{r_1, r_3\} = 1$, i.e., α is on the upper arc $C_1 \cap D_3$.

As $\alpha \in C_1$, there is $t \in \left[\frac{1}{8}, \frac{3}{8}\right]$ with $\alpha = z_1 + \frac{\sqrt{2}}{2}e^{2\pi i t}$, so by (16), we obtain

$$u_1 = e^{2\pi i \theta_1} = \sqrt{2}(\alpha - z_1)e^{-\frac{\pi i}{4}} = e^{2\pi i \left(t - \frac{1}{8}\right)}. \tag{22}$$

When $\theta_1 = \frac{p}{q}$ is an irreducible fraction, the orbit has a finite number of convergent subsequences. Therefore, we have the following result.

Theorem 2. *If for the integers $0 < p < q$, we have $\theta_1 = \frac{p}{q} \in \left[0, \frac{1}{4}\right]$ is an irreducible fraction, then $u_1 = e^{2\pi i \frac{p}{q}}$ and by Formula (10), the sequences $(a_n)_{n\geq 0}$, $(b_n)_{n\geq 0}$, $(c_n)_{n\geq 0}$, and $(d_n)_{n\geq 0}$ have subsequences which converge to the vertices of a regular $q-$gon centred at G_0 of radius $|M|$.*

Proof. In this case, we have $u_1^{nq+j} = u_1^j$ for $j = 0, \ldots, q-1$ and $u_2^n \to 0$ and $u_3^n \to 0$, so using the notations of (10) and (11), one obtains the relations

$$\begin{aligned}
\lim_{n\to\infty} a_{nq+j} &= \lim_{n\to\infty}\left(g_0 + Mu_1^{nq+j} + Nu_2^{nq+j} + Pu_3^{nq+j}\right) = g_0 + Mu_1^j \\
\lim_{n\to\infty} b_{nq+j} &= \lim_{n\to\infty}\left(g_0 + (Mi)u_1^{nq+j} + (-N)u_2^{nq+j} + (-Pi)u_3^{nq+j}\right) = g_0 + (Mi)u_1^j \\
\lim_{n\to\infty} c_{nq+j} &= \lim_{n\to\infty}\left(g_0 + (-M)u_1^{nq+j} + Nu_2^{nq+j} + (-P)u_2^{nq+j}\right) = g_0 + (-M)u_1^j \\
\lim_{n\to\infty} d_{nq+j} &= \lim_{n\to\infty}\left(g_0 + (-Mi)u_1^{nq+j} + (-N)u_2^{nq+j} + (Pi)u_3^{nq+j}\right) = g_0 + (-Mi)u_1^j,
\end{aligned} \tag{23}$$

which ends the proof. This case is depicted in Figure 6. The sequences $(a_n)_{n\geq 0}$, $(b_n)_{n\geq 0}$, $(c_n)_{n\geq 0}$, and $(d_n)_{n\geq 0}$ are plotted in Figure 7. Moreover, one can check that for $\theta_1 = 1/5$ the limit polygon is a pentagon centred at G_0, of radius $|M| \simeq 7.81$ (by (19)). $\square$

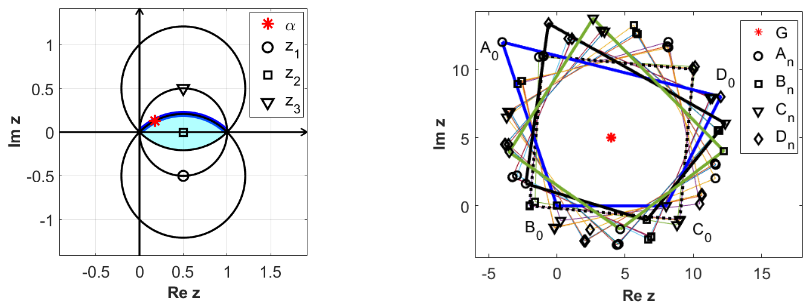

Figure 6. First 200 iterations (**right**) obtained for $\theta_1 = p/q = 1/5$ where $\alpha = z_1 + \frac{\sqrt{2}}{2}e^{2\pi i\left(\frac{1}{8}+\frac{1}{5}\right)}$ (**left**).

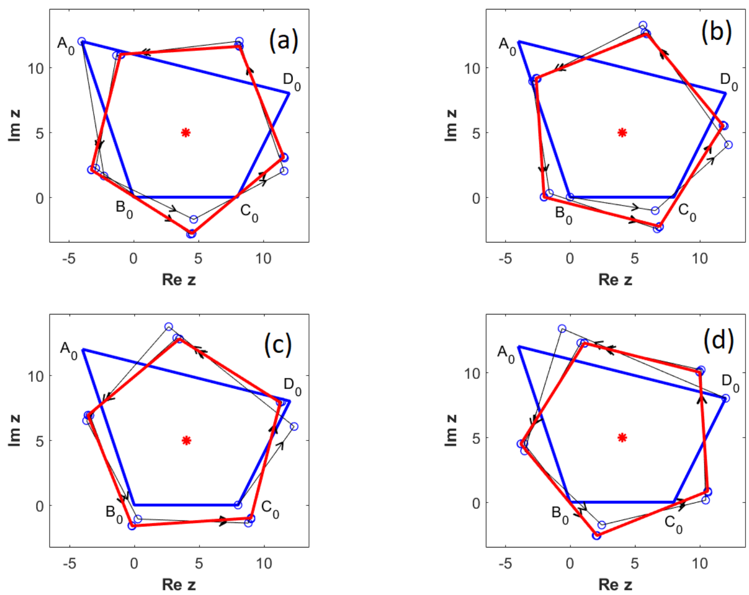

Figure 7. Iterations obtained for $\theta_1 = \frac{1}{5}$. (**a**) $(a_n)_{n=0}^{199}$; (**b**) $(b_n)_{n=0}^{199}$; (**c**) $(c_n)_{n=0}^{199}$; (**d**) $(d_n)_{n=0}^{199}$.

4.4.2. Lower Arc of C_3

Similarly, if $r_3 = \max\{r_1, r_3\} = 1$, then α is on the arc $C_3 \cap D_1$ defined by (17). Therefore, there is $t \in \left[\frac{5\pi}{8}, \frac{7\pi}{8}\right]$ with $\alpha = z_3 + \frac{\sqrt{2}}{2}e^{2\pi it}$, and by (16), we obtain

$$u_3 = e^{2\pi i\theta_3} = \sqrt{2}(\alpha - z_3)e^{\frac{\pi i}{4}} = e^{2\pi i\left(t+\frac{1}{8}\right)}. \tag{24}$$

The following result can be proved similarly to Theorem 2.

Theorem 3. *If for the integers $0 < p < q$, we have $\theta_3 = \frac{p}{q} \in \left[\frac{3}{4}, 1\right]$ is an irreducible fraction, then $u_1 = e^{2\pi i\frac{p}{q}}$ and by Formula (10), the sequences $(a_n)_{n\geq 0}$, $(b_n)_{n\geq 0}$, $(c_n)_{n\geq 0}$, and $(d_n)_{n\geq 0}$ have q subsequences convergent to the vertices of four regular $q-$gons centred at G_0 of radius $|P|$.*

The first 200 iterations obtained when $\theta_3 = \frac{5}{6}$ are presented in Figure 8.

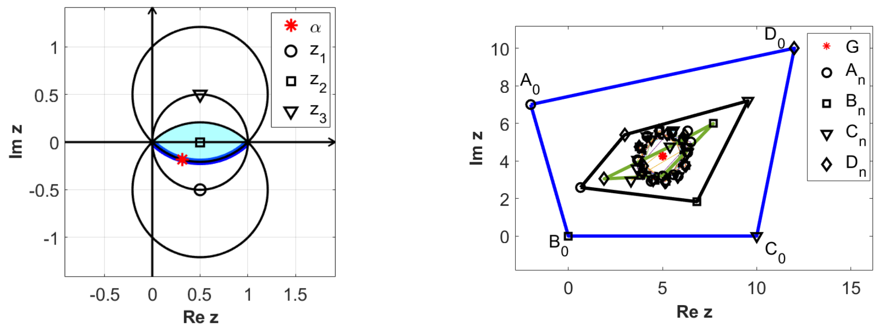

Figure 8. First 200 iterations (**right**) obtained for $\theta_3 = p/q = 5/6$ where $\alpha = z_3 + \frac{\sqrt{2}}{2}e^{2\pi i\left(\frac{5}{6}-\frac{1}{8}\right)}$ (**left**).

The sequences $(a_n)_{n\geq 0}$, $(b_n)_{n\geq 0}$, $(c_n)_{n\geq 0}$, and $(d_n)_{n\geq 0}$ are plotted in Figure 9. Similarly to (23), the limit polygon is a hexagon centred at G, which has radius $|P| = 1$.

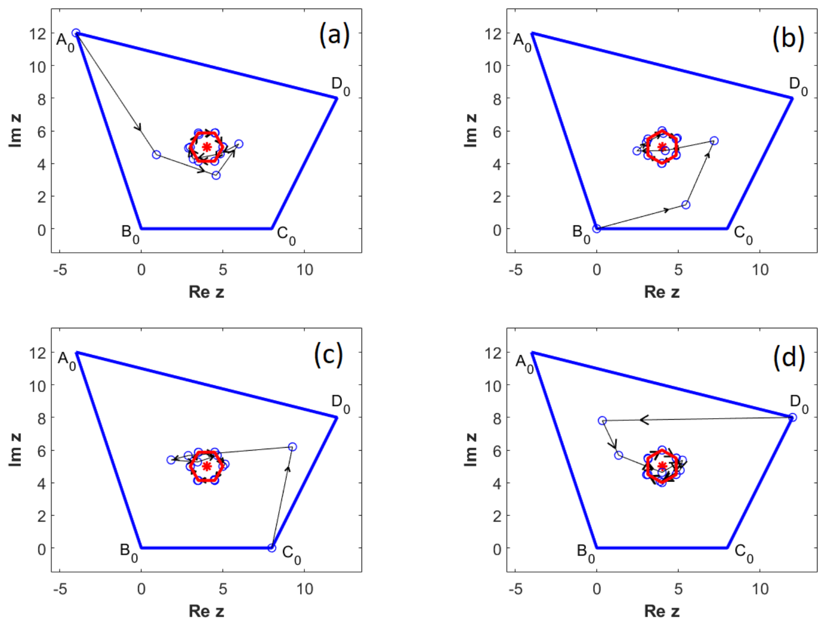

Figure 9. Iterations obtained for $\theta_3 = \frac{5}{6}$. (**a**) $(a_n)_{n=0}^{199}$; (**b**) $(b_n)_{n=0}^{199}$; (**c**) $(c_n)_{n=0}^{199}$; (**d**) $(d_n)_{n=0}^{199}$.

4.5. Dense Orbits

When $0 < \min\{r_1, r_3\} < \max\{r_1, r_3\} = 1$ but θ_1 or θ_3 are irrational modulo 2π, the orbits of $(a_n)_{n\geq 0}$, $(b_n)_{n\geq 0}$, $(c_n)_{n\geq 0}$, and $(d_n)_{n\geq 0}$ are dense within circles.

4.5.1. Upper Arc of C_1

First, assume that $0 < r_3 < r_1 = 1$, i.e., α is on the upper arc $C_1 \cap D_3$. Using the notations in (22), the following result can be deduced from Lemma 1 (d).

Theorem 4. *If $r_1 = 1$ and $\theta_1 \in \left[0, \frac{1}{4}\right]$ is irrational, then the set of limit points for each of the sequences $(a_n)_{n\geq 0}$, $(b_n)_{n\geq 0}$, $(c_n)_{n\geq 0}$, and $(d_n)_{n\geq 0}$ is the circle centred at G_0 of radius $|M|$.*

Proof. By (10), we have $a_n = g_0 + Mu_1^n + Nu_2^n + Pu_3^n$, with M, N, and P constants given by (11). Because $|u_2| < 1$, $|u_3| < 1$, we have $a_n = g_0 + Mu_1^n + z_n$, where $\lim_{n\to\infty} z_n = 0$.

Let z be an arbitrary point on the circle of centre G_0 and radius $|M|$. If $M = 0$, then $\lim_{n\to\infty} a_n = g_0$. Otherwise, denoting $z' = \frac{z-g_0}{M}$, we have $z' \in \mathcal{C}(0,1)$. Because $u_1 = e^{2\pi i\theta_1}$ with θ_1 irrational, by Lemma (1), it follows that there is a subsequence $n_1 < n_2 < \cdots$ such that $\lim_{k\to\infty} u_1^{n_k} = z'$. For $\varepsilon > 0$, one can find $K_1(\varepsilon)$ and $K_2(\varepsilon)$ such that

$$|u_1^{n_k} - z'| < \frac{1}{|M|+1}\varepsilon, \quad k \geq K_1(\varepsilon) \text{ and } |z_{n_k}| < \frac{1}{|M|+1}\varepsilon, \quad k \geq K_2(\varepsilon),$$

hence, for $k \geq \max\{K_1(\varepsilon), K_1(\varepsilon)\}$, one obtains

$$|a_{n_k} - z| = |g_0 + Mu_1^{n_k} + z_{n_k} - g_0 - Mz'| \leq |M| \cdot |u_1^{n_k} - z'| + |z_{n_k}| < \varepsilon,$$

hence $\lim_{k\to\infty} a_{n_k} = z$. This shows that z is a limit point for the sequence $(a_n)_{n\geq 0}$. Analogously, this is proved for $(b_n)_{n\geq 0}$, $(c_n)_{n\geq 0}$ and $(d_n)_{n\geq 0}$. $\square$

Figure 10 illustrates the position of α and the polygons obtained for $n = 10$ iterations, respectively, when $\alpha \in C_1 \cap D_3$. Figure 11 depicts the vertices of the original quadrilateral of affixes $(a_n)_{n\geq 0}$, $(b_n)_{n\geq 0}$, $(c_n)_{n\geq 0}$, and $(d_n)_{n\geq 0}$, and 200 iterations.

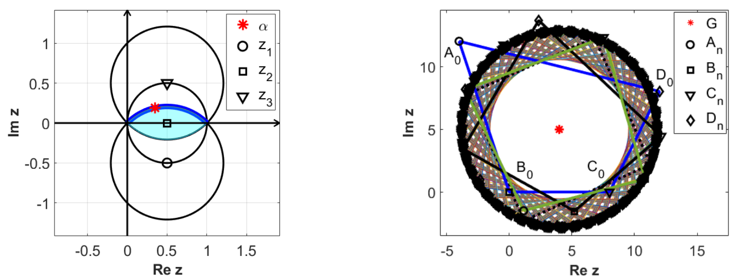

Figure 10. Orbits for $n = 10$ iterations (**right**), for $\alpha = z_1 + \frac{\sqrt{2}}{2}(\cos 1 + i \sin 1)$ (**left**).

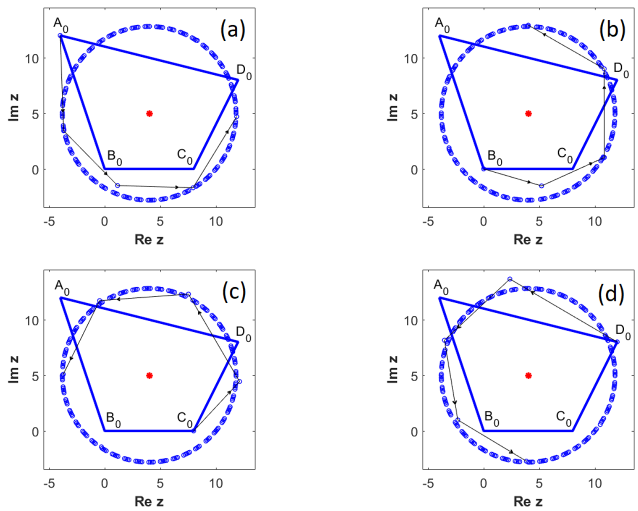

Figure 11. Orbits for $\theta_1 = \frac{1}{2\pi}$. (**a**) $(a_n)_{n\geq 0}$; (**b**) $(b_n)_{n\geq 0}$; (**c**) $(c_n)_{n\geq 0}$; (**d**) $(d_n)_{n\geq 0}$.

4.5.2. Lower Arc of C_3

When $0 < r_1 < r_3 = 1$, α is on the arc $C_3 \cap D_1$ defined by (17), as in Figure 12. Using the notations in (24), we can formulate the following result.

Theorem 5. *If $r_3 = 1$ and $\theta_3 \in \left[\frac{3}{4}, 1\right]$ is irrational, then the set of limit points for each of the sequences $(a_n)_{n\geq 0}$, $(b_n)_{n\geq 0}$, $(c_n)_{n\geq 0}$, and $(d_n)_{n\geq 0}$ is the circle centred at G_0 of radius $|P|$.*

Proof. The proof follows the similar lines as for Theorem 4, but now by (10), one has $a_n = g_0 + Mu_1^n + Nu_2^n + Pu_3^n$. Because $|u_1| < 1$, $|u_2| < 1$, we obtain $a_n = g_0 + z_n + Pu_3^n$, where $\lim_{n\to\infty} z_n = 0$. Figure 12 shows the position of α and the first $n = 10$ iterations, respectively, when $\alpha \in C_3 \cap D_1$. Figure 13 plots the vertices of the original quadrilateral of affixes $(a_n)_{n\geq 0}$, $(b_n)_{n\geq 0}$, $(c_n)_{n\geq 0}$, and $(d_n)_{n\geq 0}$, and 200 iterations. □

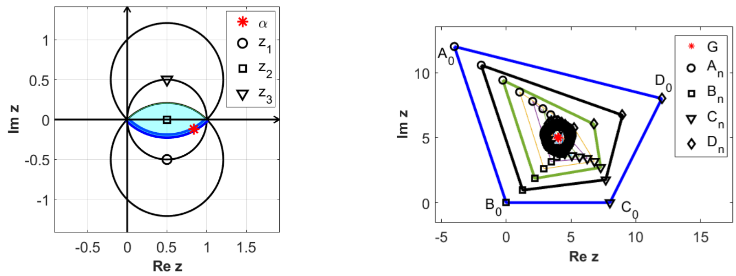

Figure 12. Dense orbits obtained after $n = 10$ iterations (**right**), generated for $\alpha = z_3 + \frac{\sqrt{2}}{2}e^{2\pi i(\frac{3}{\pi}-\frac{1}{8})}$ (**left**), when $u_3 = e^{2\pi i\theta_3}$, with $\theta_3 = \frac{3}{\pi}$.

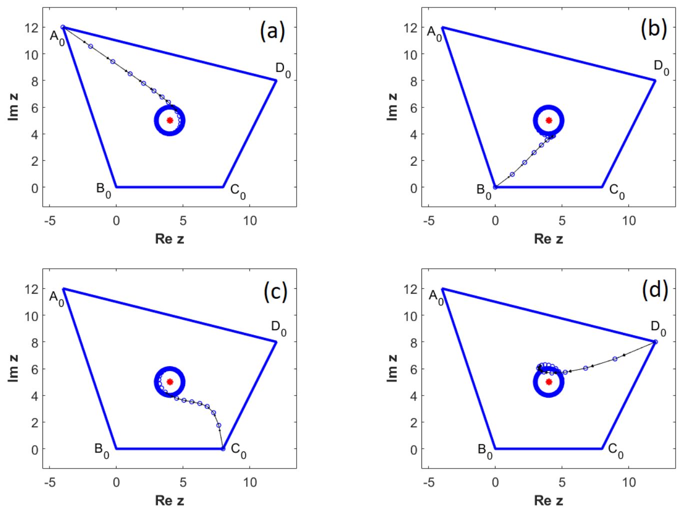

Figure 13. Orbits for $\theta_3 = \frac{3}{\pi}$. (**a**) $(a_n)_{n\geq 0}$; (**b**) $(b_n)_{n\geq 0}$; (**c**) $(c_n)_{n\geq 0}$; (**d**) $(d_n)_{n\geq 0}$.

Author Contributions: All authors claim to have contributed significantly and equally to this work. All authors have read and agreed to the published version of the manuscript.

Funding: This research was funded by "1 Decembrie 1918" University of Alba Iulia through scientific research funds.

Acknowledgments: The authors wish to thank the referees for their valuable feedback and constructive comments, which helped to improve the quality of the manuscript.

Conflicts of Interest: The authors declare no conflict of interest.

References

1. Andrica, D.; Bagdasar, O.; Marinescu, D.Ş. Dynamic geometry of Kasner triangles with a fixed weight. *Int. J. Geom.* **2022**, *11*, 101–110.
2. Kingston, J.G.; Synge, J.L. The sequence of pedal triangles. *Am. Math. Mon.* **1988**, *95*, 609–620. [CrossRef]
3. Abbot, S. Average sequences and triangles. *Math. Gaz.* **1996**, *80*, 222–224. Available online: https://www.jstor.org/stable/3620354 (accessed on 12 March 2022). [CrossRef]
4. Chang, G.Z.; Davis P.J. Iterative processes in elementary geometry. *Am. Math. Mon.* **1983**, *90*, 421–431. [CrossRef]
5. Clarke, R.J. Sequences of polygons. *Math. Mag.* **1979**, *90*, 102–105. [CrossRef]
6. Ding, J.; Hitt, L.R.; Zhang, X.-M. Markov chains and dynamic geometry of polygons. *Linear Algebra Appl.* **2003**, *367*, 255–270. [CrossRef]
7. Hitt, L.R.; Zhang, X.-M. Dynamic geometry of polygons. *Elem. Math.* **2001**, *56*, 21–37. [CrossRef]
8. Ismailescu, D.; Jacobs, J. On sequences of nested triangles. *Period. Math. Hung.* **2006**, *53*, 169–184. [CrossRef]
9. Donisi, S.; Martini, H.; Vincenzi, G.; Vitale, G. Polygons derived from polygons via iterated constructions. *Electron. J. Differ. Geom. Dyn. Syst.* **2016**, *18*, 14–31. Available online: http://www.mathem.pub.ro/dgds/v18/D18-do-b77.pdf (accessed on 7 April 2022).
10. Roeschel, O. Polygons and iteratively regularizing affine transformations. *Beitr. Algebra Geom.* **2017**, *58*, 69–79. [CrossRef]
11. Andreescu, T.; Andrica, D. *Complex Numbers from A to ... Z*, 2nd ed.; Birkhäuser: Boston, MA, USA, 2014.
12. Andrica, D.; Bagdasar, O. On the dynamic geometry of Kasner triangles with complex parameter. In Proceedings of the 7th IACMC 2022, Zarqa University, Zarqa, Jordan, 11–13 May 2022; Nature Springer: Berlin, Germany, 2022; *accepted*.
13. Bagdasar, O.; Larcombe, P.J. On the characterization of periodic complex Horadam sequences. *Fibonacci Quart.* **2013**, *51*, 28–37. Available online: https://www.fq.math.ca/Papers1/51-1/BagdasarLarcombe.pdf (accessed on 10 December 2021).
14. Andrica, D.; Bagdasar, O. *Recurrent Sequences: Key Results, Applications and Problems*; Nature Springer: Berlin, Germany, 2020.
15. Hardy, G.H.; Wright, E.M. *An Introduction to the Theory of Numbers*, 5th ed.; Oxford University Press: Oxford, UK, 1979.